Talanta 83 (2010) 262–268

Contents lists available at ScienceDirect

Talanta

journal homepage: www.elsevier.com/locate/talanta

GC/MS-based metabolomics reveals fatty acid biosynthesis and cholesterol metabolism in cell lines infected with influenza A virus

Shuhai Lin[a], Ning Liu[a,b], Zhu Yang[c], Wenjun Song[d], Pui Wang[d], Honglin Chen[d], Marianna Lucio[e], Philippe Schmitt-Kopplin[e], Guonan Chen[f], Zongwei Cai[a,*]

[a] Department of Chemistry, Hong Kong Baptist University, Hong Kong SAR, China
[b] Jilin University, Changchun, China
[c] Department of Physics, Hong Kong Baptist University, Hong Kong SAR, China
[d] State Key Laboratory for Emerging Infectious Diseases, Department of Microbiology, The University of Hong Kong, Hong Kong SAR, China
[e] Helmholtz-Zentrum Muenchen-German Research Center for Environmental Health, Institute for Ecological Chemistry, Ingolstaedter Landstrasse 1, D-85764 Oberschleißheim, Germany
[f] Ministry of Education Key Laboratory of Analysis and Detection for Food Safety, Fuzhou University, Fuzhou 350002, China

ARTICLE INFO

Article history:
Received 25 July 2010
Received in revised form
10 September 2010
Accepted 18 September 2010
Available online 24 September 2010

Keywords:
Metabolomics
Multivariate data analysis
Influenza A virus
GC/MS

ABSTRACT

Metabolomics is the downstream of systems biology and has drawn significant interest for studying the metabolic networks from cells to organisms. To profile the metabolites in two different cell lines (A549 and AGS) infected with influenza A virus, gas chromatography coupled with mass spectrometry (GC/MS) was employed. Some differentiating metabolites in the cell lines were tentatively identified using reference library, interpreted and visualized by applying principal components analysis (PCA) and cluster heat map. Consequently, metabolic flux profiling allowed the differentiation of fatty acid biosynthesis and cholesterol metabolism during viral replication in the cell lines. The change in fatty acid turnover was also observed. Metabolomics investigation also revealed the different responses between A549 and AGS cell lines to the virus infection. From the pattern recognition results, AGS cell line might be more susceptible to influenza A virus. Regarding the fact that AGS is a poorly differentiated gastric adenocarcinoma cell line whereas A549 is a relatively differentiated lung tumor one, it is speculated that viral replication might be associated with the cell differentiations.

1. Introduction

The recent H1N1 and the H5N1 avian flu virus have caused significant concerns on human health and life [1–2]. Therefore, understanding the virus infection at systems-level is of great interest [3]. Metabolomics may provide important information of the dynamics of influenza A virus and host interaction in mammalian cell settings because metabolic phenotype would be changed in the organism when gene's function is altered [4]. The phenotype for the site of action, in the metabolic network, of a silent gene could also be revealed by the "metabolic snapshots" [5].

Gas chromatography coupled with mass spectrometry (GC/MS) has a long history for global or targeted analysis in metabolomic studies for the identification and quantification of endogenous metabolites in *Escherichia coli*, rodent animal and human biofluids [6–8]. The analysis of metabolomic profiling data from GC/MS measurements usually relies on mass spectrum reference libraries such as the National Institute of Standards and Technology (NIST) for metabolite identification and tracking. The relative quantification could reveal the metabolic changes in non-targeted metabolomics study. The global metabolic profiling from GC/MS analysis has been demonstrated to be a powerful approach to elucidate the underlying metabolic mechanisms [9]. For example, the regulatory metabolic network was determined using GC/MS to reveal acute stress and chronic unpredictable mild stress in rats. Metabolic response to cold temperature (−10 °C) for 2 h delineated several major metabolic pathways including catecholamines, glucocorticoids, the tricarboxylic acid (TCA) cycle, tryptophan (nicotinate), gut microbiota metabolism, and chronic combined stress exhibited biochemical clues to depression-like symptoms validated by behavior and physiological results [10–11]. GC/MS is only suitable for the analysis of volatile and thermally stable compounds. Thus, derivatization is usually required prior to the sample injection for increasing volatility and/or improving thermal stability. Ethyl chloroformate (ECF) was preferred for the derivatization because it can simultaneously react with both the amino and the carboxylic groups rapidly at room temperature in aqueous solution instead of organic solvent. The derivatization agent has been successfully

* Corresponding author. Tel.: +852 3411 7070; fax: +852 3411 7348.
E-mail address: zwcai@hkbu.edu.hk (Z. Cai).

0039-9140/$ – see front matter © 2010 Elsevier B.V. All rights reserved.
doi:10.1016/j.talanta.2010.09.019

applied to yield volatile derivatives of amino acids and fatty acids. Therefore, its potential for global analysis of biological samples has received more and more attention [12–15].

Establishing cell models is of particular importance in understanding the metabolic mechanisms of viral replication. A549 cell line, an epithelial cell line derived from lung adenocarcinoma, has been widely applied in influenza virus strains infection [16–18]. AGS, a stomach cancer cell line, is a poorly differentiated gastric adenocarcinoma cell line. Epstein-Barr Virus (EBV) could lead to promote AGS carcinoma invasiveness, which may establish a link between EBV and the low differentiated or anaplastic status of the carcinomas that carry the virus [19–21]. The mechanism of viral replication was also investigated to accumulate more and more evidence. It should be noted that fatty acid synthase (FAS) gene product is required for de novo synthesis of the palmitate fatty acid. FAS was found to be up-regulated in not only EBV but also hepatitis C virus (HCV)-infected cells [22–23]. Accompanying the increased FAS expression, cholesterol synthesis was also enhanced in patients with HCV infection [24].

Collectively, fatty acid biosynthesis as well as cholesterol metabolism might serve the important metabolic pathways for revealing the cell metabolism which could be derailed by viral infection. In this study, GC/MS was employed for a global analysis of the dynamic courses for influenza A virus infection in A549 and AGS cell lines. Multivariate data analysis was performed for the separation and visualization of the tested cell sample sets.

2. Materials and methods

2.1.1. Chemicals

4-Chloro-DL-phenylalanine was purchased from Sigma (Sigma–Aldrich, USA). Ethyl chloroformate (ECF) was purchased from Merck (Hohenbrunn, Germany). Pyridine, anhydrous ethanol and chloroform were analytical grade from Lab-scan (Labscan Asia Co., Ltd., Bangkok, Thailand). Ultrapure water was prepared from a Milli-Q system (Millipore, USA).

2.1.2. Cell culture and virus infection

Monolayer cultures of A549 cells (ATCC CCL-185) and AGS cells (ATCC CRL-1739) were cultured in Dulbecco modified eagle medium supplemented with 10% FBS, 100 IU of penicillin G/mL and 100 mL of streptomycin sulfate/mL. Influenza A virus strain (A/Hong Kong/2108/2003, HK2108), was inoculated onto confluent monolayers of the A549 or AGS cell line at a multiplicity of infection of approximately 0.1 in 11 cm culture plates. The infected cells were harvested at four different time courses (0, 12, 24, and 48 h) by scraping followed by washing three times with PBS. For each time point, cells were cultured in quadruplicate with $\sim 1.5 \times 10^6$ cells each sample in 10-cm dish.

2.1.3. Sample preparation

The cell pellets were suspended in 200 μL of 100% methanol (−80 °C). After being thawed at room temperature, the suspensions were centrifuged 5 min at 14,000 × *g* at 4 °C. The supernatant was retained and stored at −80 °C, and a further aliquot (200 μL) of 100% methanol (−80 °C). The above procedure was repeated by adding the second aliquot of methanol to the pellet. The combined samples were dried with gentle nitrogen stream. The cell sample was diluted in 50 μL of 4-chloro-DL-phenylalanine (0.1 mg mL^{-1} in water), followed with the addition of 50 μL of anhydrous ethanol and 20 μL of pyridine. The sample solution was vortexed for 30 s, added with 50 μL of ECF for derivatization at 20.0 ± 0.5 °C, and sonicated at 40 kHz for 60 s. Extraction was then conducted using 100 μL of chloroform. The chloroform supernatant was removed through centrifugation for 5 min at 8000 × *g* at 4 °C. The derivatization and extraction were repeated with 50 μL of ECF and 100 μL of chloroform. The combined chloroform was vortexed with anhydrous sodium sulfate and clarified for 5 min at 14,000 × *g* at 4 °C.

2.1.4. GC/MS analysis

The derivatized extracts were analyzed on Agilent 6890N gas chromatography coupled with 5975B mass spectrometric detector. A 1-μL aliquot was injected into HP-5MS capillary column coated with 3% phenyl methyl siloxane (30 m × 250 μm i.d., 0.25-μm) in splitless mode. The injection temperature and the interface temperature were set to 260 °C. The temperature of quadrupole and the ion source temperature was adjusted to 150 °C and 230 °C, respectively. Initial GC oven temperature was 100 °C for 5 min, increased by 10 °C min^{-1} to 200 °C and then increased to 280 °C at a rate of 4 °C min^{-1}. Helium was the carrier gas with a flow rate of 1 mL min^{-1}. Solvent delay was set for 7 min. The measurements were made with electron impact (EI) ionization (70 eV) in the full scan mode (*m/z* 50–550). Identification of the compounds was searched against NIST library.

2.1.5. Data analysis

The GC/MS data in instrument-specific format were converted to CDF format files. The program XCMS was implemented in R language for non-linear retention time alignment, automatic integration and extraction of the peak intensities. The output tables were imported into MATLAB software R2008a (The MathWorks, Inc.), where normalization was performed prior to multivariate data analysis. Principal components analysis (PCA), cluster heat map and *z*-score plot were performed in MATLAB programming environment. Score line plots in OPLS/O2PLS model were performed in SIMCA-P software version 12.0 (Umetrics AB, Umea, Sweden). The one-way analysis of variance (one-way ANOVA) was utilized to compare the virus-infected sample sets with those of control group for up- or down-regulated metabolites. The *P*-values and *F*-values were obtained by OriginPro software version 8.0 (OriginLab, Co., MA).

The overall workflow chart for the GC/MS-based metabolic signature is illustrated in Fig. 1. Features selected based on the *P*-value and fold-change ($P \leq 0.001$ with fold-change ≥1.5 was adopted in four levels comparison) of the resulting tab delimited table generated from XCMS, then manual integrations of the peak areas were normalized by the peak area of the internal standard. The *P*-values and *F*-values of one-way ANOVA were recalculated using Bonferroni correction. The raw data was also used for OPLS/O2PLS model performance in SIMCA-P after normalization to obtain score line plots. When finishing identification of the metabolites of interest, PCA analysis, heat map display and *z*-score plot for improving visualization were also performed.

3. Results and discussion

GC/MS analysis of endogenous metabolites such as fatty acids and cholesterol in the cellular samples was conducted with the ECF derivatization. The typical total ion chromatograms of cell samples of A549 and AGS are shown in Fig. 2. The majority of individual features detected were presented in cell samples. As summarized in Table 1, about 15% of all features detected in the four sample sets of A549 or AGS cell lines showed significant changes in their relative signal intensities (defined as a $P \leq 0.001$). It should be noted that for the data with $P \leq 0.001$, only 13.0% fold-change ≥1.5 was found in A549 cell line, while up to 90.2% fold-change ≥1.5 was observed

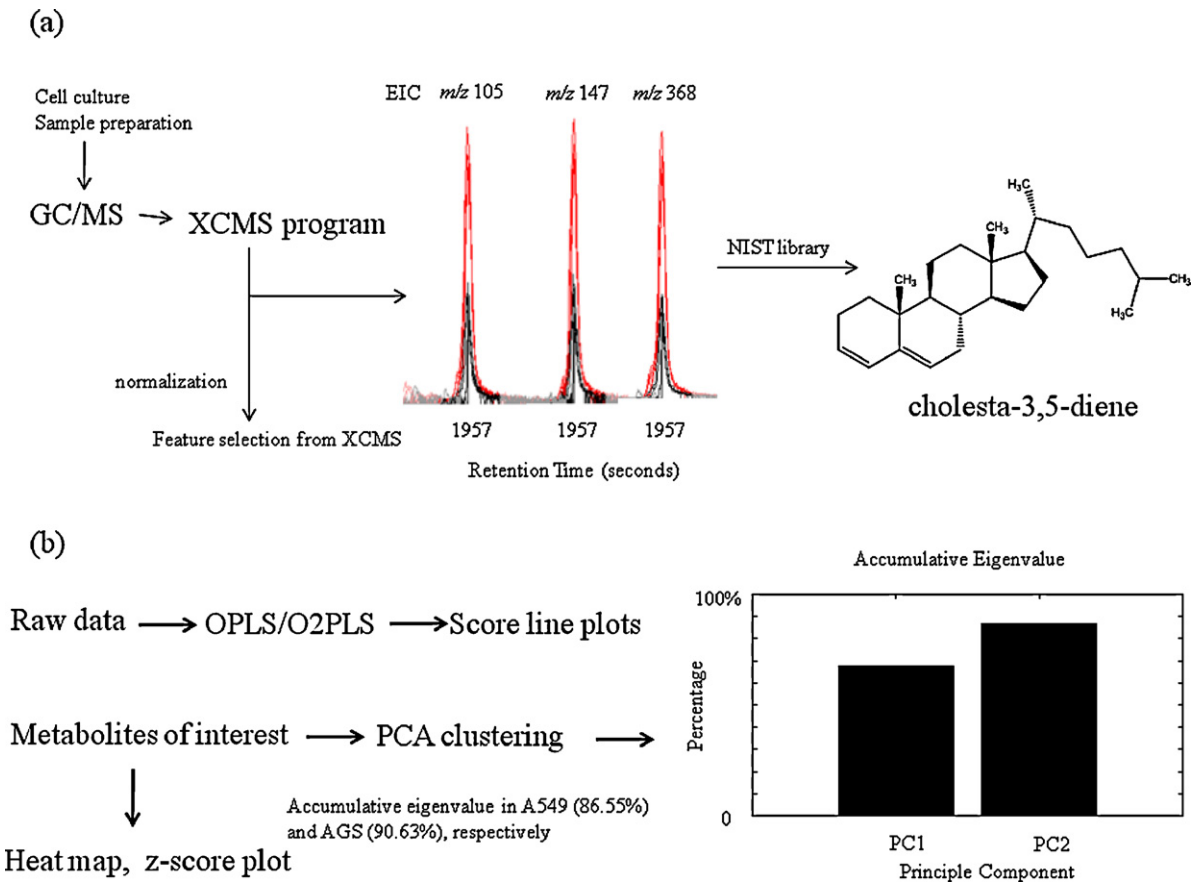

Fig. 1. Schematic diagram of the GC/MS metabolomics analytical platform. Three typical peaks of cholesta-3,5-diene generated in EI–MS were shown using XCMS program. The bar plot denotes accumulative eigenvalues in a PCA model.

in AGS cell line, suggesting that influenza A virus might pose more clear influence on AGS than A549 cells during the viral replication. A given molecule may be represented by several different features, such as the fragment ions in EI–MS analysis. Thus, we obtained a large number of features from GC/MS analysis. After the integrations of peak areas, identification of the metabolites which met our criteria (P-value ≤ 0.001 with fold-change ≥ 1.5) was conducted by searching against NIST library. F-values were also calculated for

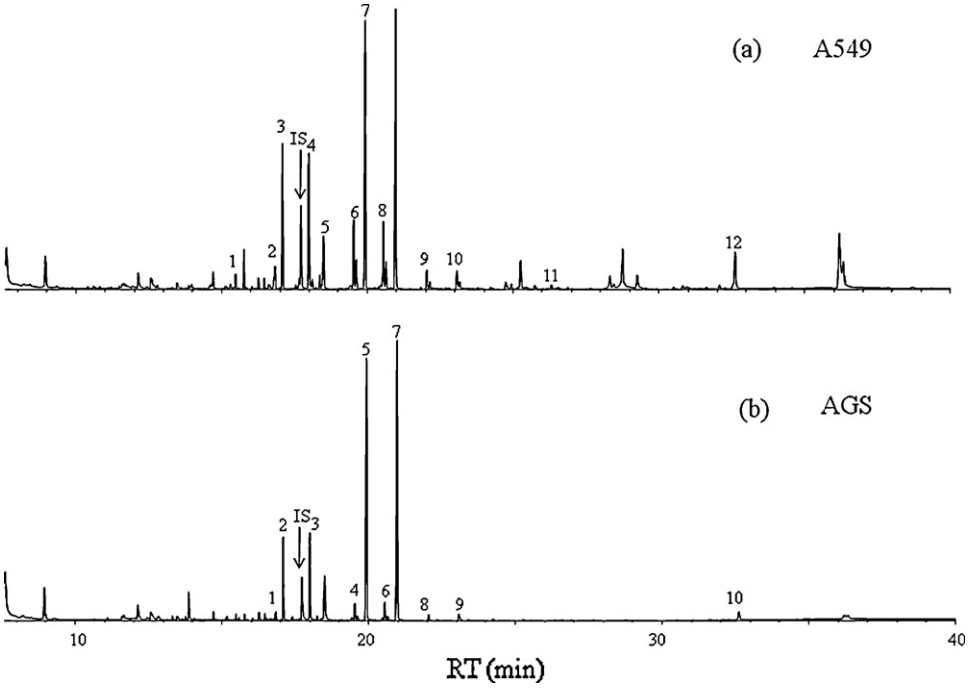

Fig. 2. Typical GC/MS chromatograms from the analysis of A549 and AGS cell lines.

Table 1
Characterization of the global metabolomic data from the GC/MS analysis.

	No. of features in A549[a]	No. of features in AGS
Total observations	841	340
Observations with $P \leq 0.001$	146 (17.4%)[b]	51 (15.0%)
Observations with $P \leq 0.001$ and fold change ≥ 1.5	19 (13.0%)[c]	46 (90.2%)

[a] Defined as an *m*/*z*-retention time pair for which a peak has been found in at least 1 group of samples in the data set; *P* values compare one uninfected group and 3 infected groups' integrated intensities.
[b] Percentage is obtained with the comparison to the "total observations".
[c] Percentage is obtained with the comparison to the "observations with $P \leq 0.001$".

Table 2
Statistical significant metabolites detected by GC/MS from A549 and AGS data sets.

Peak no. in A549	Peak no. in AGS	RT (min)	Metabolites	Match percent[a] (%)	*P* value in A549 (*F* value)[b]	*P* value in AGS (*F* value)
1		15.48	C14:0	98	3.11E−06 (35.30)	
2	1	16.82	C16:1	99	1.82E−09 (132.71)	1.24E−13 (673.30)
3	2	17.09	C15:0	98	1.74E−04 (15.93)	2.85E−06 (35.90)
4	3	17.99	C16:1	98	1.81E−04 (15.81)	2.49E−06 (36.79)
5		18.38	Octadecenal	95	9.66E−08 (66.36)	
6	4	19.52	C 18:1	99	4.60E−05 (20.98)	4.67E−08 (75.47)
7	5	19.91	C18:1	99	7.97E−04 (11.39)	2.12E−05 (24.46)
8	6	20.54	C18:1	99	1.76E−06 (39.24)	2.14E−08 (86.54)
	7	20.95	C18:1	99		3.19E−05 (22.57)
9	8	22.05	C20:4	94	8.54E−06 (29.17)	3.03E−13 (579.53)
10	9	23.07	C20:4	95	1.49E−04 (16.46)	4.04E−10 (171.74)
11		26.33	C20:4	93	2.56E−07 (55.76)	
12	10	32.62	Cholesta-3,5-diene	96	6.92E−09 (105.34)	5.30E−04 (12.50)

[a] Match percentage was obtained against NIST searching library for identification.
[b] *P* values and *F* values were generated from one-way ANOVA using Origin software (version 8.0).

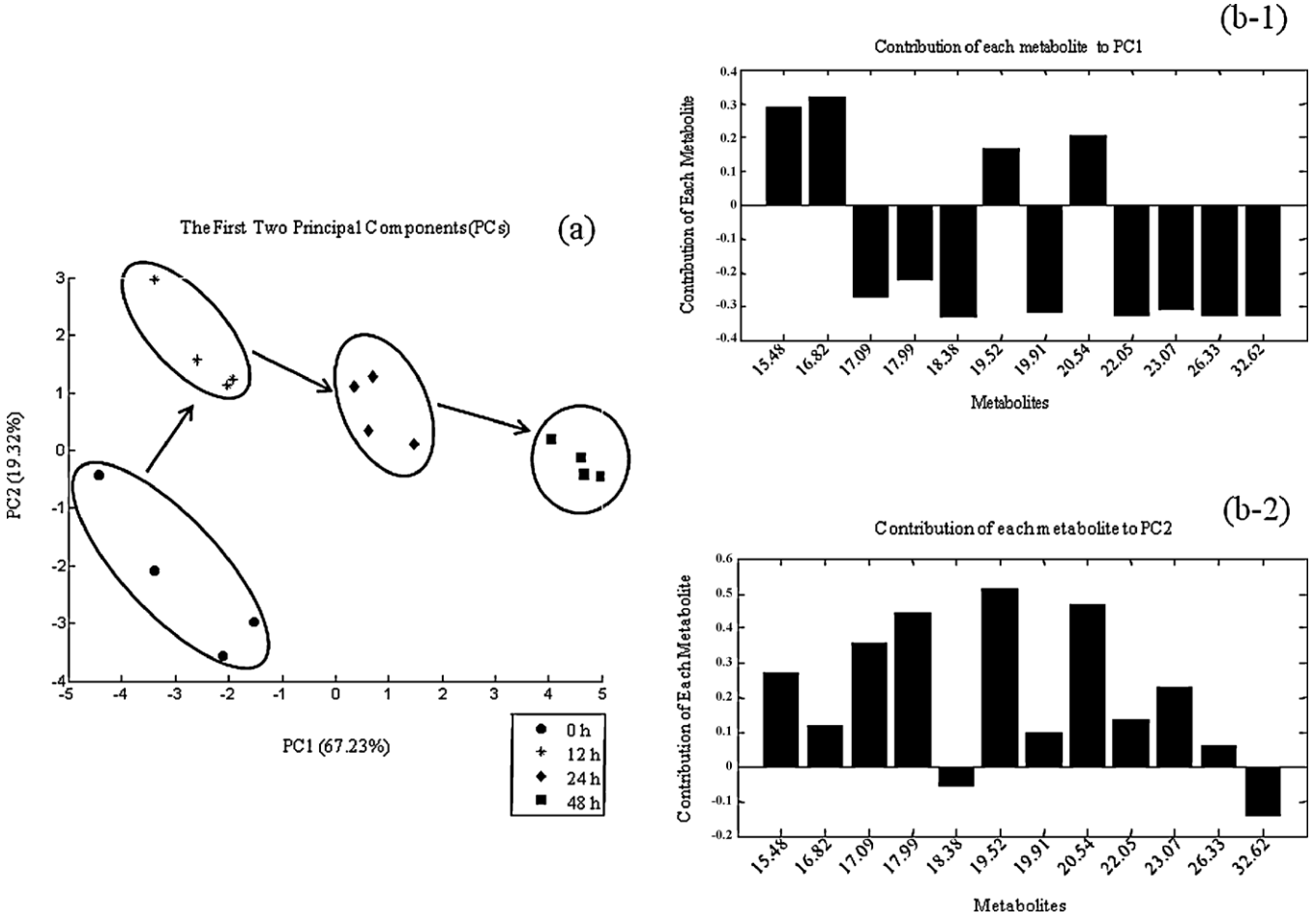

Fig. 3. PCA grouping results of A549 (a) and the contribution of each metabolite for PC1 (b-1) and PC2 (b-2).

reference and the larger *F*-value, the difference in grouped sample sets is more significant. The statistical significant compounds as the differentiating metabolites are summarized in Table 2. The data showed that most match percentages in NIST library were more than 95% and the significant differences in metabolic levels between the cell sample sets were calculated using four-level comparison.

3.1.1. Grouping and comparing viral infection in A549 and AGS cell lines

PCA was performed for the separation of various experimental groups using the differentiating metabolites after the metabolites of interest were highlighted. For the grouping virus infection in A549 cell line, PC1 accounts for 67.23% of the total variation and PC2 for 19.32% (Fig. 3). On the other hand, PC1 accounts for 62.75% of the total variation and PC2 for 27.88% in AGS cell line (Fig. 4). It is well-known that PCs are ordered by their contribution to the variance of the data set resulting in the first PC explains more of the variance in the data set than the second one. The accumulative eigenvalues of PCA were computed as 86.55% and 90.63% for A549 and AGS cell lines, respectively. In general, the first two PCs could indicate the highly efficient separation among grouped samples when accumulative eigenvalues are up to 90%. Therefore, discrimination in AGS cell line seemed to be more susceptible to viral replication in comparison to A549 cells although the two models adopted the differentiating metabolites only. Based on the PCA model, the contribution of each metabolite was exhibited in PC1 and PC2. Among the differentiating metabolites, interestingly, 8 negative contributions to PC1 in A549 cell line indicated that 66.7% metabolites was decreased by virus infection whereas 33.3% metabolites enhanced exposed by virus (4 positive contributions to PC1). Notably, 90.0% metabolites were up-regulated by viral infection in AGS cell line whereas only 1 metabolite (10.0%) was down-regulated. The results suggested that fatty acid profiling disturbed by the same virus could have different signature metabolic shifts in different cell types. For PC2, the contribution of each metabolite showed the individual variation of the cell samples, for example, those at 12 h post-infection versus the control (0 h) in PCA pattern recognition.

The trajectories in both cell lines were depicted in not only PCA model but also the score line plots. The score line plots in OPLS/O2PLS model were established using the raw data after the internal standard in both cell lines was normalized to be the same intensity. When the dataset contains numerical identities, they were selected and plotted on either axis. The score plot displayed confidence intervals corresponding to the 2 or 3 sigma limits, i.e., 2 or 3 standard deviations of the vector were displayed by default. In Figs. S1 and S2, clearer separation were obtained for the time-dependent AGS cell line than that of A549 cell line, which is consisting with the global characterization of the profiling data (Table 1) and the PCA analysis results using the differentiating metabolites. To improve the visualization, these profiles were displayed as cluster heat maps (Figs. S3 and S4) and *z*-score plots (Figs. S5 and S6). The heat map represented the unsupervised hierarchical clustering of the data grouped by sample type (columns), which also enabled visualization of the up- or down-regulation of each metabolite. It should be noted that the fold change of cell lines in heat map was observed (−2 to 2 in A549 versus −3 to 3

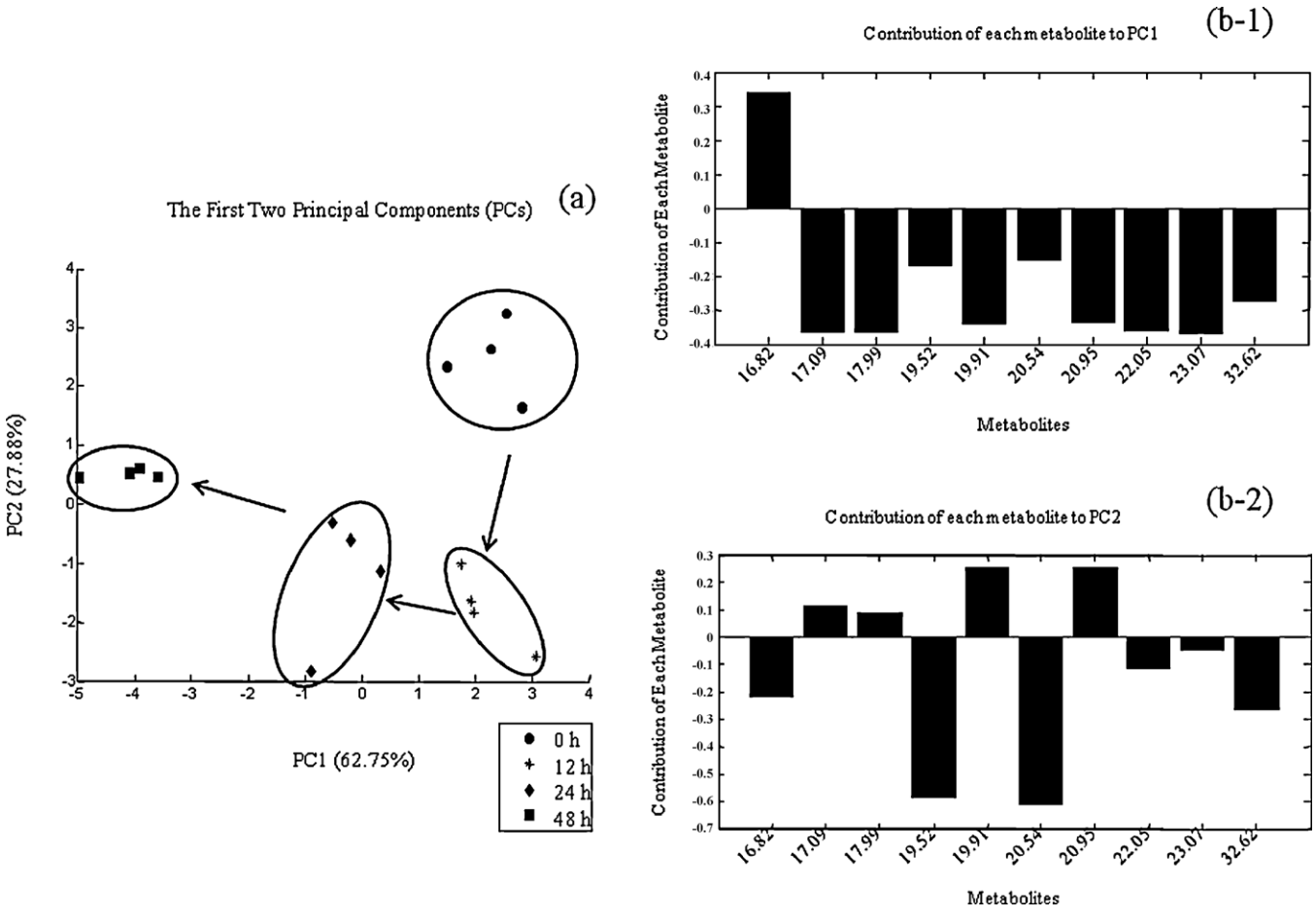

Fig. 4. PCA grouping results of AGS (a) and the contribution of each metabolite for PC1 (b-1) and PC2 (b-2).

in AGS). More importantly, only 48 h group was separated from the samples but the distribution of other samples could not be easily recognized in A549 experiment. In contrast, discrimination of four groups in AGS was much clearer. It should be noted that, however, the trees for clusters showed grouping metabolites as well as samples. By taking the trees for the metabolites, both of the cell lines are divided into two clusters. The *z*-score plots reflected robust metabolic alterations in different time courses during virus infection (*z*-score range: −20 to 10 in A549; *z*-score range: −40 to 80 in AGS). Notably, fatty acid C16:1 at RT 16.82 min was increased in concentration markedly whereas another fatty acid C20:4 at RT 22.05 min was pronouncedly decreased in concentration of AGS cells exposed by influenza A virus. In summary, the results implied that the virus infection posed more influence on AGS, although less peaks were detected by GC/MS in AGS than A549 cell experiment (Table 1 and Fig. 2).

For the further understanding of difference between A549 and AGS cell lines infected by influenza A virus, the statistical box plots were calculated based on the criteria: the shared differentiating metabolites in both cell lines and the same regulations induced by virus in PC1 of PCA model. The opposite contributions to PC1 clearly reflected the different fluctuations in concentration. Therefore, seven metabolites were highlighted as the box plots (Fig. 5). Interestingly, the significant changes of these metabolites (virus-infected cells at 12, 24 and 48 h versus non-infected cells, respectively) exhibited different change tendencies between A549 and AGS cell lines. From the dynamic metabolic shifts of influenza A virus and host interaction in cultured mammalian cells, the sample of 12 h was an important time point to show some metabolites turnover, such as C15:0 at RT 17.09 min, C16:1 at RT 17.99 min in A549 cell line, which could also be observed in the trajectories of PCA pattern recognitions. Additionally, the C16:1 at RT 16.82 min, C20:4 at RT 22.05 min and cholesta-3,5-diene at RT 32.62 min were shown distinct alterations by virus exposure between the two cell lines, which was consistent with the observations of *z*-score plots.

3.2. Fatty acid biosynthesis and cholesterol metabolism as the targets

The obtained results from GC/MS measurement demonstrated 12 and 10 differentiating metabolites in A549 and AGS, respectively, indicating that influenza A virus altered fatty acid biosynthesis and cholesterol metabolism in the cell lines. Cholesta-3,5-diene and fatty acids were measured as the statistically significant metabolite candidate in both cell lines. Cholesterol is a combination of a sterol and a lipid to build block for the cell membranes. It has been reported that fatty acid biosynthesis is an important metabolic pathway in virus infection. Infection with human cytomegalovirus (HCMV) notably increased the flux through the tricarboxylic acid cycle and its efflux to the fatty acid biosynthesis pathway using liquid chromatography coupled with tandem mass spectrometry [25]. Cholesta-3,5-diene, which can be considered as an extremely non-polar dehydration product of cholesterol, has been recognized in animal tissues, resulted from non-enzymatic formation of cholesterol [26]. Similarly, the infection of mouse L cells by encephalomyocarditis virus modified membrane permeability and the alteration of permeability to translation inhibitors was observed after the infection of different mammalian cell lines

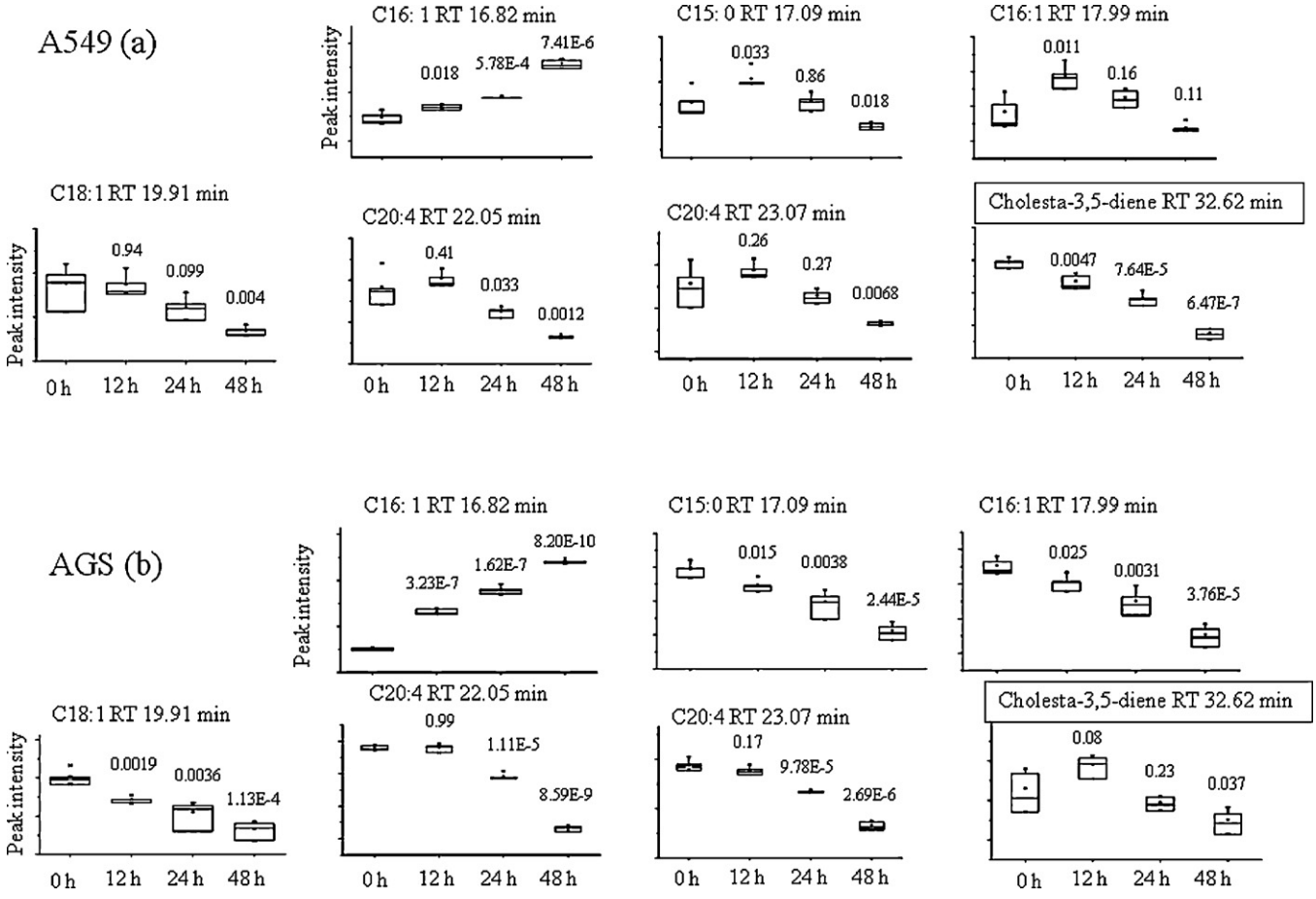

Fig. 5. Box plots of the time-dependent metabolic changes of virus-infection in A549 (a) and AGS (b). The peak intensities of cell sample sets after infection (12, 24 and 48 h) were used for calculations compared to the start (0 h) and each *P*-value was filled on the box plot with metabolite name and its retention time in GC/MS chromatogram.

with different viruses such as vesicular stomatitis virus and Semliki Forest virus, two lipid-enveloped RNA-containing viruses [27]. More recently, RNA viruses were found to selectively exploit specific elements of the host to form specialized organelles where cellular phosphoinositide lipids played a key role in viral replication [28]. The alteration of fatty acids and dehydration product of cholesterol demonstrated that fatty acid biosynthesis and cholesterol metabolism could be induced by virus infection in A549 and AGS cell lines, which were associated with intracellular metabolic perturbation and cell membrane permeability.

Only one cell type in the G_0 stage of the cell cycle was used for the previous investigation [25], we adopted and compared two kinds of cell lines: A549 and AGS. A549 is a relatively differentiated tumor cell line, featuring the phenotype of alveolar type II cells by its surfactant-producing ability, whereas AGS adenocarcinoma cells might represent an undifferentiated form of gastric epithelia [29]. Surprisingly, the highly efficient pattern recognition techniques for either raw data or the differentiating metabolites determined that AGS cell line might be more susceptible to viral replication than A549. It was reported previously that the poorly differentiated cells generally showed an enhanced sensitivity to H-1 virus attack compared to well-differentiated cells [30]. The enhanced sensitivity of the poorly differentiated cells versus the well-differentiated gastric cancer cells might be partly related to the enhanced capacity of poorly differentiated cells for NS1 protein production and accumulation. Thus, our results indicated that the metabolic signature shifts in the cells infected with influenza A virus might be associated with differentiated stages of the cells. Furthermore, we found that cholesta-3,5-diene as the differentiating metabolite in A549 cell line, which surprisingly, was more distinct in its trajectory during the infection between the virus and host engaging in a dynamic duet when compared to AGS. Thereby we speculated that viral replication revealed from metabolic phenotyping and associated with differentiation of the cells might be, at least partially, due to fatty acid biosynthesis. This speculation was basically consistent with the metabolic signature in a model of adipocyte differentiation [31]. The speculation, however, should be exploited further with the relationship between the kinetic metabolic snapshots, such as fatty acid profiling, and differentiation of other cells (e.g. 3T3-L1 cell line) infected by virus.

4. Conclusions

Metabolic profiling revealed viral replication in A549 and AGS cell lines altered fatty acid biosynthesis and cholesterol metabolism, suggesting that virus would rely on the metabolic network of their cellular hosts to provide energy and that viral infection would modify cellular architecture and physiology, such as cell membrane permeability. The different responses to influenza A virus replication were highlighted with the efficient pattern recognition methods. Regarding the differentiation of the two cell lines, the results indicated that metabolic shifts were more significantly affected in the relatively lower differentiated cell line.

Acknowledgements

The authors would like to thank the National Nature Sciences Foundation of China (20928005) for the financial support.

Appendix A. Supplementary data

Supplementary data associated with this article can be found, in the online version, at doi:10.1016/j.talanta.2010.09.019.

References

[1] D. Butler, Nature 458 (2009) 1082–1083.
[2] J. Cohen, Science 324 (2009) 870–871.
[3] H. Kitano, Science 295 (2002) 1662–1664.
[4] P.N. Benfey, T. Mitchell-Olds, Science 320 (2008) 495–497.
[5] L.M. Raamsdonk, B. Teusink, D. Broadhurst, N. Zhang, A. Hayes, M.C. Walsh, J.A. Berden, K.M. Brindle, D.B. Kell, J.J. Rowland, H.V. Westerhoff, K van Dam, S.G. Oliver, Nat. Biotechnol. 19 (2001) 45–50.
[6] D. Oursel, C. Loutelier-Bourhis, N. Orange, S. Chevalier, V. Norris, C.M. Lange, Rapid Commun. Mass Spectrom. 21 (2007) 3229–3233.
[7] S.H. Lee, H.M. Woo, B.H. Jung, J. Lee, O.S. Kwon, H.S. Pyo, M.H. Choi, B.C. Chung, Anal. Chem. 79 (2007) 6102–6110.
[8] H. Wu, R. Xue, L. Dong, T. Liu, C. Deng, H. Zeng, X. Shen, Anal. Chim. Acta 648 (2009) 98–104.
[9] Z. Tang, M.V. Martin, F.P. Guengerich, Anal. Chem. 81 (2009) 3071–3078.
[10] X. Wang, M. Su, Y. Qiu, Y. Ni, T. Zhao, M. Zhou, A. Zhao, S. Yang, L. Zhao, W. Jia, J. Proteome Res. 6 (2007) 3449–3455.
[11] X. Wang, T. Zhao, Y. Qiu, M. Su, T. Jiang, M. Zhou, A. Zhao, W. Jia, J. Proteome Res. 8 (2009) 2511–2518.
[12] Y. Qiu, M. Su, Y. Liu, M. Chen, J. Gu, J. Zhang, W. Jia, Anal. Chim. Acta 583 (2007) 277–283.
[13] J. Duan, B. Hu, J. Mass Spectrom. 44 (2009) 605–612.
[14] J. Peris-Vicente, J.V. Gimeno Adelantado, M.T. Carbo, R.M. Castro, F.B. Reig, J. Chromatogr. A 1101 (2006) 254–260.
[15] X. Gao, E. Pujos-Guillot, J.F. Martin, P. Galan, C. Juste, W. Jia, J.L. Sebedio, Anal. Biochem. 393 (2009) 163–175.
[16] M. Noteborn, H. Arnheiter, L. Richter-Mann, H. Browning, C. Weissmann, J. Interferon Res. 7 (1987) 657–669.
[17] C.K. Fong, M.K. Lee, B.P. Griffith, J. Clin. Microbiol. 38 (2000) 4660–4662.
[18] J. Barenfanger, C. Drake, T. Mueller, T. Troutt, J. O'Brien, K. Guttman, J. Clin. Virol. 22 (2001) 101–110.
[19] J. Kassis, A. Maeda, N. Teramoto, K. Takada, C. Wu, G. Klein, A. Wells, Int. J. Cancer 99 (2002) 644–651.
[20] J. Nishikawa, C. Kiss, S. Imai, K. Takada, K. Okita, G. Klein, L. Szekely, Int. J. Cancer 107 (2003) 597–602.
[21] J.L. Ryan, R.J. Jones, S.H. Elmore, S.C. Kenney, G. Miller, J.C. Schroeder, M.L. Gulley, Intervirology 52 (2009) 8–16.
[22] Y. Li, J. Webster-Cyriaque, C.C. Tomlinson, M. Yohe, S. Kenney, J. Virol. 78 (2004) 4197–4206.
[23] W. Yang, B.L. Hood, S.L. Chadwick, S. Liu, S.C. Watkins, G. Luo, T.P. Conrads, T. Wang, Hepatology 48 (2008) 1396–1403.
[24] M. Nakamuta, R. Yada, T. Fujino, M. Yada, N. Higuchi, M. Tanaka, M. Miyazaki, M. Kohjima, M. Kato, T. Yoshimoto, N. Harada, A. Taketomi, Y. Maehara, M. Koga, T. Nishinakagawa, M. Nakashima, K. Kotoh, M. Enjoji, Int. J. Mol. Med. 24 (2009) 825–828.
[25] J. Munger, B.D. Bennett, A. Parikh, X.J. Feng, J. McArdle, H.A. Rabitz, T. Shenk, J.D. Rabinowitz, Nat. Biotechnol. 26 (2008) 1179–1186.
[26] R.J. Cenedella, L.L. Linton, C.P. Moore, Biochem. Biophys. Res. Commun. 186 (1992) 1647–1655.
[27] L. Carrasco, Virology 113 (1981) 623–629.
[28] N.Y. Hsu, O. Ilnytska, G. Belov, M. Santiana, Y.H. Chen, P.M. Takvorian, C. Pau, H. van der Schaar, N. Kaushik-Basu, T. Balla, C.E. Cameron, E. Ehrenfeld, F.J. van Kuppeveld, N. Altan-Bonnet, Cell 141 (2010) 799–811.
[29] W. Kang, O. Nielsen, C. Fenger, J. Madsen, S. Hansen, I. Tornoe, P. Eggleton, K.B. Reid, U. Holmskov, Clin. Exp. Immunol. 130 (2002) 449–458.
[30] Z.H. Ran, J. Liu, Y. Feng, J. Zou, S.D. Xiao, Chin, J. Dig. Dis. 5 (2004) 93–97.
[31] L.D. Roberts, S. Virtue, A. Vidal-Puig, A.W. Nicholls, J.L. Griffin, Physiol. Genomics 39 (2009) 109–119.